



**HAL**  
open science

## Safety, Biodistribution, and Dosimetry of 123I-6-Deoxy-6-Iodo-D-Glucose, a Tracer of Glucose Transport, in Healthy and Diabetic Volunteers

Alex Calizzano, Pascale Perret, Marie-Dominique Desruet, Mitra Ahmadi,  
Ghislaine Reboulet, Loïc Djaileb, Gérald Vanzetto, Daniel Fagret, Gilles  
Barone-Rochette, Catherine Ghezzi

► **To cite this version:**

Alex Calizzano, Pascale Perret, Marie-Dominique Desruet, Mitra Ahmadi, Ghislaine Reboulet, et al.. Safety, Biodistribution, and Dosimetry of 123I-6-Deoxy-6-Iodo-D-Glucose, a Tracer of Glucose Transport, in Healthy and Diabetic Volunteers. *Clinical Nuclear Medicine*, 2019, 44 (5), pp.386-393. 10.1097/RLU.0000000000002510 . inserm-02440453

**HAL Id: inserm-02440453**

**<https://inserm.hal.science/inserm-02440453>**

Submitted on 3 Feb 2020

**HAL** is a multi-disciplinary open access archive for the deposit and dissemination of scientific research documents, whether they are published or not. The documents may come from teaching and research institutions in France or abroad, or from public or private research centers.

L'archive ouverte pluridisciplinaire **HAL**, est destinée au dépôt et à la diffusion de documents scientifiques de niveau recherche, publiés ou non, émanant des établissements d'enseignement et de recherche français ou étrangers, des laboratoires publics ou privés.

# Clinical Nuclear Medicine

## Safety, biodistribution, and dosimetry of 123I-6-deoxy-6-iodo-D-glucose (6DIG), a tracer of glucose transport, in healthy and diabetic volunteers

--Manuscript Draft--

<b>Manuscript Number:</b>	CNM-D-18-01222R1
<b>Full Title:</b>	Safety, biodistribution, and dosimetry of 123I-6-deoxy-6-iodo-D-glucose (6DIG), a tracer of glucose transport, in healthy and diabetic volunteers
<b>Article Type:</b>	Original Article
<b>Keywords:</b>	123I-6DIG; Glucose transport; biodistribution; dosimetry; Insulin Resistance
<b>Corresponding Author:</b>	Pascale Perret, PhD INSERM La Tronche, Rhones-Alpes FRANCE
<b>Corresponding Author Secondary Information:</b>	
<b>Corresponding Author's Institution:</b>	INSERM
<b>Corresponding Author's Secondary Institution:</b>	
<b>First Author:</b>	Pascale Perret, PhD
<b>First Author Secondary Information:</b>	
<b>Order of Authors:</b>	Pascale Perret, PhD Alex Calizzano, MD Marie-Dominique Desruet, PharmD, PhD Mitra Ahmadi, PhD Ghislaine Reboulet, Medical Physicist Loïc Djaileb, MD Gérald Vanzetto, MD, PhD Daniel Fagret, MD, PhD Gilles Barone-Rochette, MD, PhD Catherine Ghezzi, PhD
<b>Order of Authors Secondary Information:</b>	
<b>Abstract:</b>	<p>Purpose: Insulin resistance (IR) is a key feature of the metabolic syndrome and type 2 diabetes which noninvasive assessment is not currently allowed by any methodology. We previously validated an iodinated tracer of glucose transport (6DIG) and a new methodology for the in vivo quantification of cardiac IR in rodents. The aim of this study was to investigate the safety, biodistribution, and radiation dosimetry of this method using 123I-6DIG in 5 healthy and 6 diabetic volunteers.</p> <p>Methods: The collection of adverse events (AE) and medical supervision of vital parameters and biological variables allowed the safety evaluation. Biodistribution was studied by sequentially acquiring whole-body images at 1, 2, 4, 8 and 24 hours post-injection. The total number of disintegrations in each organ normalized to the injected activity was calculated as the area under the time-activity curves. Dosimetry calculations were performed using OLINDA/EXM.</p> <p>Results: No major AE were observed. The average dose corresponding to the two injections of 123I-6DIG used in the protocol was 182.1±7.5 MBq. A fast blood clearance of 123I-6DIG was observed. The main route of elimination was urinary, with &gt;50% of urine activity over 24hrs. No blood or urine metabolite was detected. 123I-6DIG accumulation mostly occurred in elimination organs such as kidneys and liver. Mean radiation dosimetry calculations indicated an effective whole-body absorbed</p>

dose of  $3.35 \pm 0.57$  mSv for the whole procedure.  
Conclusions:  $^{123}\text{I}$ -6DIG was well tolerated in human with a dosimetry profile comparable to that of other commonly used iodinated tracers, thereby allowing further clinical development of the tracer.

January, 11<sup>th</sup> 2019

**Manuscript reference #CNM-D-18-01222:** “Safety, biodistribution, and dosimetry of 123I-6-deoxy-6-iodo-D-glucose (6DIG), a tracer of glucose transport, in healthy and diabetic volunteers”. Alex Calizzano, Pascale Perret, Marie-Dominique Desruet, Mitra Ahmadi, Ghislaine Reboulet, Loïc Djaileb, Gérald Vanzetto, Daniel Fagret, Gilles Barone-Rochette and Catherine Ghezzi.

Dear Editor,

Please find enclosed the revised version of our manuscript #CNM-D-18-01222 together with a point-by-point response to the comments of the reviewer. We greatly appreciate the helpful feedback from the reviewer: Figure 5 has been modified according to its remark, and the English has been polished up. We hope that our manuscript is now suitable for publication in Clinical Nuclear Medicine.

**Author contributions:** AC and PP wrote the manuscript and contributed equally to its elaboration. AC, PP, MDD, GV, DF, GBR and CG designed the studies. AC, LD, GV, GBR, DF acquired the clinical data. GR managed all the dosimetry procedure and calculations. MDD and MA performed radiolabeling as well as all quality controls and the stability evaluation. PP performed the statistical analysis. AC, PP, GR, LD, MA, GV, DF, GBR and CG analyzed and interpreted the data. GBR and CG supervised equally this work. All the authors critically revised and approved the final version of the manuscript.

Thank you for your kind consideration of our revised manuscript.

Sincerely,

Pascale Perret, PhD (corresponding author)

**Manuscript reference #CNM-D-18-01222:** “Safety, biodistribution, and dosimetry of  $^{123}\text{I}$ -6-deoxy-6-iodo-D-glucose (6DIG), a tracer of glucose transport, in healthy and diabetic volunteers”.

The authors would like to thank the reviewer for their kind and helpful comments.

1) As suggested by the reviewer we managed to find someone able to polish up the English. We hope that now the manuscript is suitable for publication.

2) As mentioned by the reviewer, a letter was missing on the legend of Figure 5, we modified this legend and we can now read “Stomach” instead of “Stomac”.

**Title:** Safety, biodistribution, and dosimetry of  $^{123}\text{I}$ -6-deoxy-6-iodo-D-glucose (6DIG), a tracer of glucose transport, in healthy and diabetic volunteers.

**Authors:**

Alex Calizzano<sup>1\*</sup>, MD, Pascale Perret<sup>1\*</sup>, PhD, Marie-Dominique Desrues<sup>1</sup>, PharmD-PhD, Mitra Ahmadi<sup>1</sup>, PhD, Ghislaine Reboulet<sup>2</sup>, Medical Physicist, Loïc Djaileb<sup>1</sup>, MD, Gérald Vanzetto<sup>1</sup>, MD-PhD, Daniel Fagret<sup>1</sup>, MD-PhD, Gilles Barone-Rochette<sup>1\*</sup>, MD-PhD, and Catherine Ghezzi<sup>1\*</sup>, PhD

<sup>1</sup> Univ. Grenoble Alpes, INSERM, CHU Grenoble Alpes, LRB, 38000 Grenoble, France.

<sup>2</sup> CHU Grenoble Alpes, Department of Nuclear Medicine, 38000 Grenoble, France.

\* Authors equally contributed.

**Corresponding author:** Pascale Perret

Laboratoire Radiopharmaceutiques Biocliniques (LRB)

INSERM UMR\_S1039

Faculté de Médecine de Grenoble

38700 La Tronche

France

Telephone: +33.4.76.63.71.02

Fax: +33.4.76.63.71.42

Email: [pascale.perret@univ-grenoble-alpes.fr](mailto:pascale.perret@univ-grenoble-alpes.fr)

**Short title:** Biodistribution and dosimetry of 6DIG.

**Disclosures.** This work was funded by the ANR-06-TecSan-005-01-GLUCIMAG grant.

Authors have no conflict of interest to declare.

## **Acknowledgments**

We thank the staff of the Center of Clinical Investigation (CIC) and of the Department of Nuclear Medicine of Grenoble Hospital (CHUGA).

Safety, biodistribution, and dosimetry of  $^{123}\text{I}$ -6-deoxy-6-iodo-D-glucose (6DIG), a tracer of glucose transport, in healthy and diabetic volunteers.

**Abstract:**

**Purpose:** Insulin resistance (IR) is a key feature of the metabolic syndrome and type 2 diabetes which noninvasive assessment is not currently allowed by any methodology. We previously validated an iodinated tracer of glucose transport (6DIG) and a new methodology for the *in vivo* quantification of cardiac IR in rodents. The aim of this study was to investigate the safety, biodistribution, and radiation dosimetry of this method using  $^{123}\text{I}$ -6DIG in 5 healthy and 6 diabetic volunteers.

**Methods:** The collection of adverse events (AE) and medical supervision of vital parameters and biological variables allowed the safety evaluation. Biodistribution was studied by sequentially acquiring whole-body images at 1, 2, 4, 8 and 24 hours post-injection. The total number of disintegrations in each organ normalized to the injected activity was calculated as the area under the time-activity curves. Dosimetry calculations were performed using OLINDA/EXM.

**Results:** No major AE were observed. The average dose corresponding to the two injections of  $^{123}\text{I}$ -6DIG used in the protocol was  $182.1 \pm 7.5$  MBq. A fast blood clearance of  $^{123}\text{I}$ -6DIG was observed. The main route of elimination was urinary, with >50% of urine activity over 24hrs. No blood or urine metabolite was detected.  $^{123}\text{I}$ -6 DIG accumulation mostly occurred in elimination organs such as kidneys and liver. Mean radiation dosimetry calculations indicated an effective whole-body absorbed dose of  $3.35 \pm 0.57$  mSv for the whole procedure.

**Conclusions:**  $^{123}\text{I}$ -6DIG was well tolerated in human with a dosimetry profile comparable to that of other commonly used iodinated tracers, thereby allowing further clinical development of the tracer.

**Keywords:**  $^{123}\text{I}$ -6DIG, Glucose transport, Biodistribution, Dosimetry, Insulin Resistance.

## INTRODUCTION

Insulin resistance (IR) as partially characterized by a defect in insulin-stimulated glucose transport in insulin-sensitive tissues is a key feature of the metabolic syndrome, which also involves obesity, hypertension, an impairment in carbohydrate metabolism, and dyslipidemia with elevated triglyceridemia and decreased high density lipoproteins (HDL) levels.<sup>1-3</sup> The presence of the metabolic syndrome is strongly associated with an increased occurrence of coronary artery disease and heart failure in type 2 diabetic (T2D) patients as well as non-diabetic individuals. The public health challenge represented by the metabolic syndrome is best exemplified by its elevated prevalence (15 – 25%) in Western countries.<sup>4</sup> However, the routine clinical assessment of IR is currently not allowed by any methodology with the euglycemic hyperinsulinemic clamp technique remaining the gold-standard with the widely acknowledged limitations of complexity and duration precluding its clinical routine use.<sup>5</sup> Simpler indexes based on fasting glycemia and insulinemia such as the homeostasis model assessment (HOMA) or the quantitative insulin sensitivity check index (QUICKI) have been proposed but lack accuracy and informativeness.<sup>6-8</sup> Furthermore, such indexes are limited to global IR and do not provide any tissue-specific IR data. <sup>18</sup>F-2-fluoro-2-deoxy-D-glucose (FDG) or <sup>11</sup>C-3-O-methyl-D-glucose (3-OMG) and positron emission tomography imaging have been proposed for the regional assessment of IR with limitations similar to those described above since the methodology still requires to perform an euglycemic hyperinsulinemic-clamp as well.<sup>9,10</sup>

We previously validated the 6-deoxy-6-iodo-D-glucose (6DIG) as an iodinated tracer of glucose transport with a biological behavior similar to that of 3-OMG.<sup>11,12</sup> We demonstrated the *in vivo* feasibility of IR assessment with <sup>123/125</sup>I-6DIG in mice and rats<sup>13,14</sup> and then developed an experimental protocol allowing the assessment of cardiac IR in rats without the need for an euglycemic hyperinsulinemic-clamp.<sup>15</sup> The aim of the present study was to

evaluate the safety, biodistribution and dosimetry of the  $^{123}\text{I}$ -6DIG injection in healthy and diabetic volunteers in order to proceed with the clinical translation of the methodology previously validated preclinically.

## **MATERIALS AND METHODS**

### **Radiopharmaceutical preparation**

Iodine was purchased from IBA/CIS Bio International (sodium iodide-123 for labeling of radiopharmaceuticals as carrier free iodine in alkaline solution; 3,700 MBq/mL). 6DIG and NaI (4  $\mu\text{g}/\text{mL}$ , acetone solution) were obtained as active pharmaceutical ingredients from ERAS Labo (Saint-Nazaire-Les-Eymes, France). Sterile saline (NaCl 0.9%) and water for injection were purchased from B. Braun Medical. Methanol and acetonitrile for quality controls were of analytical grade and were obtained from Carlo Erba. Radioiodinated 6DIG was prepared through an isotopic exchange method as previously described;<sup>14</sup> and modified for clinical use as follows: radiopharmaceutical was prepared by hospital radiopharmacy in a grade A hot cell placed in a grade C environment. All vials were provided with a lead shield for radiation protection. 6DIG (5 mg) was dissolved in 1 mL solution NaI/acetone and added to sodium iodide-123 (259 MBq, 70  $\mu\text{L}$ ). The solution was heated to 95°C for one hour. After cooling to room temperature, acetone was removed by evaporation at 80°C for 10 minutes and then an additional 15 minutes after adding 100  $\mu\text{L}$  sterile water. The residue was dissolved in 1 mL sterile water and the reaction solution was purified by anion exchange chromatography (cartridge OASIS Max Waters) using 0.9% NaCl as eluent to remove free iodine-123. The volume was adjusted to 8 mL with 0.9% NaCl. Subsequently, the solution was transferred through 2 sterile filters (0.2  $\mu\text{m}$ , Sartorius) into a sealed glass vial.

### **Quality controls**

A small aliquot of the final product was used for quality controls: appearance of the solution, pH, identity of radionuclide and of radiolabeled compound, radionuclide and radiochemical purity, level of chemical impurities, residual solvents, specific activity, bacterial endotoxins, and sterility. Analyses were performed according to European Pharmacopoeia. The identification of the product, chemical and radiochemical purity were determined by high-performance liquid chromatography (HPLC) with ultraviolet (UV) detection. The column used was a C18 spherisorb 4.6x150 mm column (Waters). The mobile phase was pure water, flow was 1 mL/min, and UV detection was performed at  $\lambda=254$  nm. The radiochemical purity was also determined by high-performance thin layer chromatography (HPTLC) on aluminum thin-layer chromatography plates, coated with silicagel 60 (F254, Merck) that was developed with acetonitrile/methanol 95/5 vol/vol. Tryptone Soya Broth and Thioglycollate broth with resazurin (Biomérieux) were used to confirm the absence of bacterial growth. The level of residual acetone was determined by gas chromatography. Tests on bacterial endotoxins, sterility and residual acetone were performed after product utilization.

### **Study population**

The study was approved by the institutional review board, local ethics committee, and all volunteers signed an informed consent form after receiving a thorough explanation of the study by a qualified physician. The clinical trial registration number of this study was NCT01493934. Before participating, each volunteer had medical and laboratory examinations to verify inclusion criteria. Initially twelve patients (age range, 35-60 years) consisting in 6 healthy volunteers (3 nonlactating women using contraception or post-menopausal and 3 men) and 6 patients with T2D (1 nonlactating women using contraception and 5 men) were included in this study. The inclusion criteria for healthy volunteers were as follows:  $20 \text{ kg/m}^2 < \text{body mass index (BMI)} < 25 \text{ kg/m}^2$ , waist circumference  $< 94$  cm for male and  $< 80$  cm for woman, fasting blood glucose between 3.8 and 5.8 mmol/L, fasting insulin level between 3

and 13  $\mu\text{IU/mL}$ , glycated hemoglobin (HbA1c) < 6%, total cholesterol < 2 g/L, low density lipoproteins (LDL) < 1.6 g/L, HDL > 0.4 g/L for male and > 0.5 g/L for woman, triglycerides level < 1.5 g/L. The inclusion criteria for diabetic volunteers were as follows: stable T2D with no ketoacidosis sign during the last month, HbA1c between 6 and 8%, treated only with Metformin or diet. All volunteers with a past history of myocardial infarction, acknowledged coronary artery disease, heart rhythm disorders, severe hypertension, stroke, epilepsy, pituitary surgery, disease likely to reduce the ability of absorption, diffusion and elimination of  $^{123}\text{I}$ -6DIG, treatment that could interfere with glucose metabolism or other chronic disease were excluded.

The first healthy volunteer was excluded from the study following the first  $^{123}\text{I}$ -6DIG injection because of a high thyroid iodine-123 retention which led to the subsequent thyroid saturation using potassium iodide before radiotracer injection in all volunteers (amendment accepted).

### **Protocol design and imaging acquisition**

Any treatment was stopped at least 48 hours before the  $^{123}\text{I}$ -6DIG study. A potassium iodide tablet (130 mg) was then given to all the remaining volunteers (n=11) the evening before the study, and another tablet was provided 12-24 hours later. After an 8h-fast, a cannula was placed in the arm of each subject and  $\sim 92.5$  MBq of  $^{123}\text{I}$ -6DIG were administered intravenously (IV) as a bolus. Dynamic images were obtained (2 sec-image) during 15 minutes using a  $\gamma$ -camera (INFINIA, General Electrics) with parallel-hole, low-energy and high-resolution collimator (H2505TJ, GE) and a 128x128 matrix in order to study glucose transport under basal / fasting conditions. Insulin was then administered in accordance with the gold-standard, routine clinical procedure for dynamic stimulation of the hypothalamic-pituitary-adrenal (HPA) axis (Actrapid<sup>®</sup>, 0.1 IU/kg for healthy volunteers, 0.15-0.20 IU/kg for diabetic volunteers).<sup>14</sup> Five minutes after the insulin bolus,  $^{123}\text{I}$ -6DIG injection and image acquisition were performed again as described above in order to study insulin-stimulated

glucose transport. Static whole-body images (12 cm/min, 1024x512 matrix) were then obtained at 1, 2, 4, 8, and 24 hours after the first 6DIG injection in order to determine the biodistribution of the tracer over time. Intra-individual reproducibility was assessed by submitting two healthy volunteers to an additional injection of  $^{123}\text{I}$ -6DIG (~92.5 MBq) in the basal / fasting state without IHT 14 days following the completion of the protocol.

Carbohydrate-rich juice or food was systematically proposed 15 minutes after insulin injection, or over the course of image acquisition in order to prevent severe hypoglycemia.

### **Safety**

***Clinical follow-up.*** A full clinical examination including blood pressure, heart rate measurements and ECG was performed at the inclusion visit as well as 24 hours and 7 days following completion of the 6DIG protocol. Volunteers stayed under strict medical supervision during the whole hour following insulin injection in order to detect any clinical symptom of hypoglycemia.

Adverse effects (AE) were monitored at each step of the study and collected using the volunteers' account prior to being graded according to the Medical Dictionary for Regulatory Activities (MedDRA) System Organ Class.

***Biologic follow-up.*** A cannula was inserted intravenously in the arm not used for  $^{123}\text{I}$ -6DIG injection. Blood samples were obtained upon the day of inclusion as well as 5 min before the injection and 24 hours & 7 days after. Electrolytes, complete blood count (CBC), platelet counts, prothrombin and activated partial thromboplastin time (APTT), glycemia, insulinemia, HbA1c, cholesterol, HDL, LDL, triglycerides, aspartate transaminase (AST), alanine transaminase (ALT), creatine phosphokinase, lactate dehydrogenase (LDH), alkaline phosphatase, bilirubin, gamma GT, urea, and creatinine were assayed. A pregnancy test was performed in women before  $^{123}\text{I}$ -6DIG injection and during the last visit. Special attention was

paid to the follow-up of the insulin test with serial blood glucose and insulin measurements at 0.5, 1, 2, 5, 10, 15, 20, 25, 30, 45, 60, 75 minutes and 24 hours.

### **Pharmacokinetics and metabolites**

***Radioactivity in blood and metabolites.*** Venous blood sampling was performed at 0.5, 1, 2, 5, 10, 15, 20, 25, 30, 45 minutes; 1, 4, 8 and 24 hours post injection (pi) in order to evaluate blood  $^{123}\text{I}$ -6DIG kinetics and the potential presence of metabolites. Plasma activity was assessed using a gamma well-counter (COBRA-5003, Packard) following centrifugation. Results were expressed as a percentage of the injected activity (%IA) after correction for  $^{123}\text{I}$  decay. Plasma samples were also analyzed by radio-HPLC for the detection of potential metabolites.

***Radioactivity in urine and metabolites.*** Urinary  $^{123}\text{I}$ -6DIG activity was assessed using samples collected between 0-2, 2-4, 4-8, and 8-24 hours after injection and radioactivity assessment as described above. Results were expressed as a %IA after correction for  $^{123}\text{I}$  decay. Urine samples were also analyzed by radio-HPLC.

***Radioactivity in the feces.*** Feces were collected for 24 hours and radioactivity was counted using a gamma-counter ARIES.

### **Biodistribution and dosimetry**

Regions of interest (ROIs) were manually placed on organs presenting a visible uptake of  $^{123}\text{I}$ -6DIG, on whole-body images, in an anterior and posterior incidence face, to generate time-activity curves for each organ for 24 hours. The first image acquisition was performed before the first micturition so that the total whole-body activity computed from image analysis corresponded to the IA.  $^{123}\text{I}$ -6DIG time-activity evolution for each organ was expressed as %IA after correction for  $^{123}\text{I}$  decay.

The estimation of radiation doses for the organs and the whole-body effective dose were obtained using OLINDA/EXM software (Vanderbilt University, USA). ROIs were manually

placed on the following organs: heart, lungs, thyroid, salivary glands, brain, liver, bladder, kidney, spleen, muscle, gonads, intestine, and stomach. Geometric means for each pair of decay and attenuation corrected conjugate ROIs were calculated by multiplying the net anterior counts by the net posterior counts and taking the square root of the product. Decay correction was necessary to compare each time point to the original whole-body activity level. The fraction of IA at each time point was then estimated by dividing the corrected geometric mean number of counts in each ROI by the net geometric mean number of counts in the initial whole-body image. The total number of disintegrations in each organ normalized to IA, subsequently referred to as the residence time (RT):  $\text{kBq}\cdot\text{h}\cdot\text{kBq}^{-1}$  was calculated as follows:  $\text{RT} = (\text{AUC} \times V_{\text{organ}}) / \text{IA}$ ; where AUC is the area under the curve of the non-decay-corrected time-activity curve, and  $V_{\text{organ}}$  is the tabulated organ volume as used in OLINDA/EXM.<sup>17</sup> The internal radiation dosimetry was evaluated through the RTs for the visible organs in each subject provided as an input to OLINDA/EXM. Absorbed doses were then estimated for each subject using the standardized adult male or female models in OLINDA/EXM, and effective doses were based on the tissue weighting factors (WT) from ICRP 60.<sup>18</sup>

### **Statistical analysis.**

All results were presented as mean  $\pm$  standard deviation (SD). For the two groups of volunteers, AE' frequency was expressed as number and the corresponding percentage, and statistical comparison was performed using Fisher's exact test. Fisher F-test was employed for variances comparisons. Student *t*-test and Mann & Whitney U-test were employed for paired/unpaired datasets with equal variances and unpaired datasets with unequal variances, respectively. Differences were considered significant for  $P < 0.05$ .

## **RESULTS**

### **<sup>123</sup>I-6DIG preparation**

The radiochemical purity after radiolabeling was  $97.4 \pm 1.6\%$ . Unbound I-123 always represented less than 5% in each injected solution. Typical  $^{123}\text{I}$ -6DIG HPLC profiles are displayed in Figure 1A.

### **Volunteers characteristics**

The main differences between the two groups of volunteers at the time of inclusion are presented in Table 1. As expected, fasting glucose, insulin, HbA1c levels and HOMA indexes were significantly higher in diabetic than in healthy volunteers while QUICKI indexes were significantly lower.

### **Safety**

The injection of  $^{123}\text{I}$ -6DIG was well tolerated with no significant modification of vital signs, clinical exam or ECG. All recorded AE are shown in Table 2. Ten out of the eleven volunteers reported at least one slight and transient AE. However, no severe AE were recorded. In total, 19 AE were notified including headache, somnolence (36.8%) or discomfort associated with venous catheters including injection site hemorrhage or hematoma (26.3%) (Table 2). The number of subjects reporting at least one AE was comparable between the two groups of volunteers ( $P=0.999$ ).

### **Pharmacokinetics, clearance and metabolites**

**Plasma.** As previously observed in rodents,<sup>12,13</sup> plasma clearance and blood clearance were superimposable (data not shown). Circulating  $^{123}\text{I}$ -6DIG activity increased twice during the complete protocol following each bolus-injection prior to quickly decreasing (Fig. 2A).  $^{123}\text{I}$ -6DIG blood clearance was fast with only  $5.7 \pm 2.2\%$  IA remaining 5 minutes after the first injection.  $^{123}\text{I}$ -6DIG blood clearance was also evaluated on the second part of the protocol following insulin stimulation, between 25 min and 24 h (Fig. 2B). The data were best fitted with a double exponential curve giving a blood circulating half-life of  $^{123}\text{I}$ -6DIG estimated around 7 minutes for the fast part of the curve and a blood circulating half-life around 8 hours

for the slow part of the curve. No  $^{123}\text{I}$ -6DIG metabolite was observed in any subjects throughout the study (Fig. 1B). Tracer de-iodination occurred from 30 min to 4 h post-injection (pi) as indicated by the percentage of free iodine-123 increasing from  $18.7 \pm 6.9\%$  at 30 min to  $50.8 \pm 34.0\%$  at 1 h pi and  $85.7 \pm 28.5\%$  at 4 h pi. Plasma tracer activity was below the detection threshold of radio-HPLC afterwards.

**Urine.**  $^{123}\text{I}$ -6DIG elimination mainly occurred from the urinary route. Indeed, cumulated urinary  $^{123}\text{I}$ -6DIG activity represented  $30.2 \pm 14.2\%$  IA at 8 hours following injection and  $51.7 \pm 18.2\%$  IA at 24 hours (Fig. 3). No  $^{123}\text{I}$ -6DIG metabolite was observed during the 24h-follow up.  $^{123}\text{I}$ -6DIG represented  $64.6 \pm 8.0\%$  of the radioactive profile between 0-2 h,  $54.6 \pm 18.4\%$  between 2-4 hours, and nearly 0% afterwards due to the increasing corresponding presence of free iodine-123.

**Feces.**  $^{123}\text{I}$ -6DIG was predominantly found in urine and only  $0.044 \pm 0.055\%$  IA was recovered in the feces during the 24h-follow up.

### **Biodistribution**

Representative images at different time points following  $^{123}\text{I}$ -6DIG injection are shown in Figure 4. The comparison of  $^{123}\text{I}$ -6DIG biodistribution between healthy and diabetic volunteers on one hand and male and female volunteers on the other hand indicated no significant differences. At 1-2 h pi,  $^{123}\text{I}$ -6DIG was mainly detectable in organs involved in glucose metabolism such as the liver or in its elimination such as the kidneys and bladder (Fig. 4 and Fig. 5).  $^{123}\text{I}$ -6DIG activity decreased over time in these organs. Thyroid and stomach activity were observed, which could be attributed to the biodistribution of free iodine-123 (Fig. 4 and Fig. 5). A modest cardiac activity of  $^{123}\text{I}$ -6DIG was observed ( $1.8 \pm 1.4\%$  IA at 1 h pi).

### **Dosimetry**

The mean RTs for healthy and diabetic volunteers are summarized in Table 3. The organs receiving the highest absorbed dose were the thyroid, stomach wall, urinary bladder wall, and osteogenic cells (Table 3 and 4). The total effective dose was slightly significantly higher in women than in men,  $2.01 \cdot 10^{-2} \pm 2.41 \cdot 10^{-3}$  mSv/MBq *versus*  $1.65 \cdot 10^{-2} \pm 2.63 \cdot 10^{-3}$  mSv/MBq respectively ( $P < 0.05$ ). No difference was observed between the total effective dose in healthy and diabetic volunteers ( $1.97 \cdot 10^{-2} \pm 3.10 \cdot 10^{-3}$  mSv/MBq *vs*  $1.69 \cdot 10^{-2} \pm 2.79 \cdot 10^{-3}$  mSv/MBq, respectively,  $P = 0.12$ ). No intra-individual difference was observed.

The total effective dose resulting from the evaluation of all volunteers was  $1.81 \cdot 10^{-2} \pm 0.31 \cdot 10^{-2}$  mSv/MBq, corresponding to an effective whole-body absorbed dose of  $3.35 \pm 0.57$  mSv for a total IA of ~185 MBq (Table 5).

## DISCUSSION

The main objective of this study was to evaluate the safety of  $^{123}\text{I}$ -6DIG injection in humans. The administration of  $^{123}\text{I}$ -6DIG was well tolerated with no major AE being recorded. Minor inconveniences were reported, with some appearing to be independent of  $^{123}\text{I}$ -6DIG administration such as bruise at the point of draining, urinary infection, urinary incontinence. In addition, the causal link between additional AE such as nausea & headache and  $^{123}\text{I}$ -6DIG injection was equivocal. Insulin administration was well tolerated as well, with transient hypoglycemia inducing minor clinical symptoms such as hunger and fatigue which were quickly addressed by sugar ingestion. One diabetic volunteer presented a transient rise of ASAT and ALAT values with normal values being observed upon the last visit of the study. Biodistribution of  $^{123}\text{I}$ -6DIG indicated no organ-specific retention with a low rate of tissue extraction as indicated by the blood kinetics of the tracer. The major part of  $^{123}\text{I}$ -6DIG activity was found in organs of elimination such as the stomach, bladder, and liver. Cardiac uptake was low with less than 2% IA at 1h-pi. Previous *in vitro* or *in vivo* studies in rodents indicated

that the cellular uptake of 6DIG through glucose transporters (GLUTs) was fast.<sup>11,12,14,15</sup> In addition, <sup>123</sup>I-6DIG may leave the cell through GLUTs as well since it is not metabolized. The net flux of tracer will therefore depend on its concentration gradient between the blood and tissue compartments *in vivo*, with a concentration equilibrium being reached quickly following injection. Such *in vivo* kinetics account for the lack of <sup>123</sup>I-6DIG specific organ retention.

As previously observed in animals, <sup>123</sup>I-6DIG excretion mainly occurred through the urinary tract with ~60% of the injected activity being eliminated at 24 hours following injection. A weak yet significant thyroid retention was observed due to the presence of a low circulating fraction of free iodine-123 in the injected solution ( $2.66 \pm 1.59\%$ ), which increased upon injection due to additional *in vivo* de-iodination. Thyroid saturation using potassium iodide was therefore performed as usually done when using iodinated radiotracers.

The whole-body effective dose ~3.35 mSv reached following completion of the 2 tracer injections was comparable to that observed for previously described routine clinical procedures.

## **CONCLUSION**

The tracer of glucose transport <sup>123</sup>I-6DIG was previously validated in rodents for the assessment of cardiac IR. The present study reporting a phase I clinical trial provided the *in vivo* kinetics of the tracer in humans and indicated good tolerance and a favorable dosimetry of the tracer. Further clinical studies are warranted to assess the potential of the tracer for the clinical assessment of IR.

## REFERENCES

1. Biddinger SB, Kahn RR. From mice to men: insights into the insulin resistance syndromes. *Annu Rev Physiol.* 2006;68:123-158.
2. Reaven GM. Historical perspective why syndrome X? From Harold Himsworth to the insulin resistance syndrome. *Cell Metab.* 2005;1:9-14.
3. Miranda PJ, DeFronzo RA, Califf RM, et al. Metabolic syndrome: definition, pathophysiology, and mechanisms. *Am Heart J.* 2005;149:20-32.
4. Eckel RH, Grundy SM, Zimmet PZ. The metabolic syndrome. *Lancet.* 2005;365:1415-1428.
5. Radziuk J. Insulin sensitivity and its measurement: structural commonalities among the methods. *J Clin Endocrinol Metab.* 2000;85:4426-4433.
6. Singh B and Saxena A. Surrogate markers of insulin resistance: A review. *World J Diabetes.* 2010;1(2):36-47.
7. Muniyappa R, Lee S, Chen H, et al. Current approaches for assessing insulin sensitivity and resistance in vivo: advantages, limitations, and appropriate usage. *Am J Physiol Endocrinol Metab.* 2008;294:E15-26.
8. Liu R, Christoffel KK, Brickman WJ, et al. Do Static and Dynamic Insulin Resistance Indices Perform Similarly in Predicting Pre-diabetes and Type 2 Diabetes? *Diabetes Res Clin Pract.* 2014;105(2):245-250.
9. Bertoldo A, Peltoniemi P, Oikonen V, et al. Kinetic modeling of [<sup>18</sup>F]FDG in skeletal muscle by PET: a four-compartment five-rate-constant model. *Am J Physiol Endocrinol Metab.* 2001;281:524-536.
10. Bertoldo A, Price J, Mathis C, et al. Quantitative assessment of glucose transport in human skeletal muscle: dynamic positron emission tomography imaging of [O-methyl-<sup>11</sup>C]3-O-methyl-D-glucose. *J Clin Endocrinol Metab.* 2005;90:1752-1759.

11. Henry C, Koumanov F, Ghezzi C, et al. [<sup>123</sup>I]-6-deoxy-6-iodo-D-glucose (6DIG), a potential tracer of glucose transport. *Nucl Med Biol.* 1997;24:527-534.
12. Henry C, Tanti J-F, Grémeaux T, et al. Characterization of 6-deoxy-6-iodo-D-glucose: A potential new tool to assess glucose transport. *Nucl Med Biol.* 1997;24:99-104.
13. Perret P, Ghezzi C, Mathieu J-P, et al. Assessment of insulin sensitivity *in vivo* in control and diabetic mice with a radioactive tracer of glucose transport: [<sup>125</sup>I]-6-deoxy-6-iodo-D-glucose. *Diabetes Metab Res Rev.* 2003;19:306-312.
14. Perret P, Slimani L, Briat A, et al. Assessment of insulin resistance in fructose-fed rats with <sup>125</sup>I-6-deoxy-6-iodo-D-glucose, a new tracer of glucose transport. *Eur J Nucl Med Mol Imaging.* 2007;34:734-744.
15. Briat A, Slimani L, Perret P, et al. In vivo assessment of cardiac insulin resistance by nuclear probes using an iodinated tracer of glucose transport. *Eur J Nucl Med Mol Imaging.* 2007;34:1756-1764.
16. Erturk E, Jaffe CA, Barkan AL. Evaluation of the integrity of the hypothalamic-pituitary-adrenal axis by insulin hypoglycemia test. *Clin Endocrinol Metab.* 1998;83:2350-2354.
17. Stabin MG, Sparks RB, Crowe E. OLINDA/EXM: the second-generation personal computer software for internal dose assessment in nuclear medicine. *J Nucl Med.* 2005;46:1023-1027.
18. 1990 recommendations of the International Commission on Radiological Protection. ICRP publication 60. *Ann ICRP.* 1991;21:1-201.

## Figures legends:

**FIGURE 1.** HPLC profiles of  $^{123}\text{I}$ -6DIG (A) after radiolabeling in saline, and (B) 15 minutes post-injection in plasma. The first peak represents free iodine. The double-peak represents both  $\alpha$  and  $\beta$  forms of the molecule.

**FIGURE 2.** (A) Plasma activity of  $^{123}\text{I}$ -6DIG between 0 and 24 hours with a disruption of the X-axis between 80 and 400 minutes to visualize the two  $^{123}\text{I}$ -6DIG bolus-injections during the first part of the protocol (cardiac IR assessment). (B) Plasma clearance of 6DIG between 25 minutes and 24 hours, double-exponential curve fit ( $r^2=0.98$ ). Mean  $\pm$  SD, n=11.

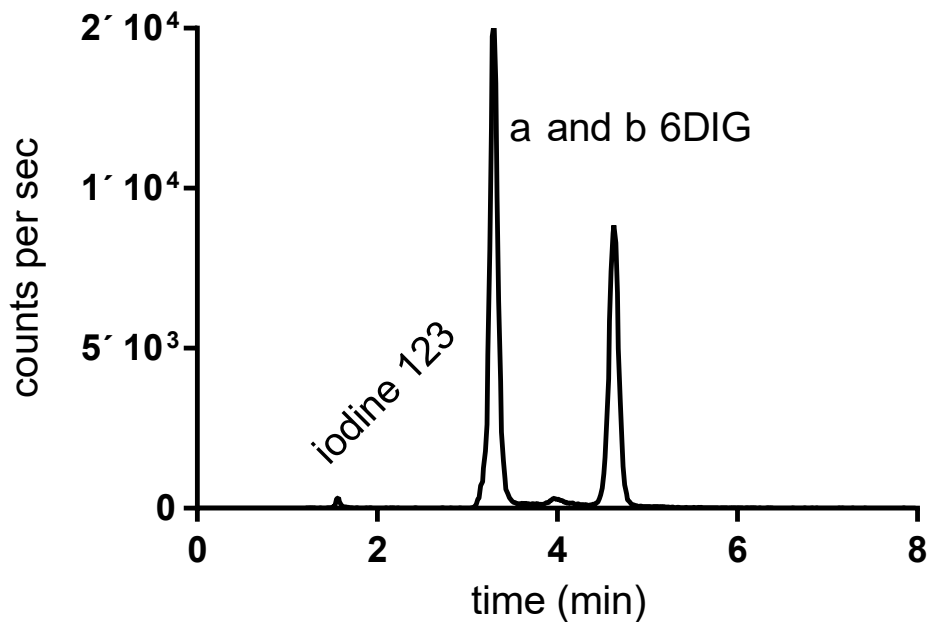
**FIGURE 3.** Cumulative urinary clearance of  $^{123}\text{I}$ -6DIG in the first 24 hours after injection. Mean  $\pm$  SD, n=10; IA: injected activity.

**FIGURE 4.** Representative examples of anterior whole-body scans 1, 2, 4, 8 and 24 hours after  $^{123}\text{I}$ -6DIG injection.

**FIGURE 5.** Time-activity curves from the major organs observable on nuclear images over a 24h-period after  $^{123}\text{I}$ -6DIG injection. Mean  $\pm$  SD (error bars are shown both side for kidneys and 1-sided for clarity for the others).

Figure 1

**A**



**B**

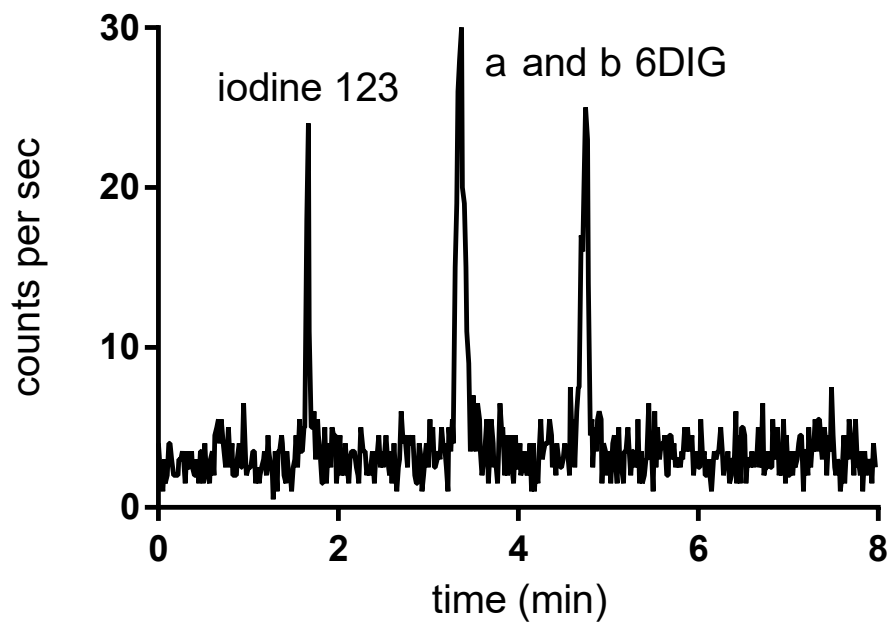


Figure 2

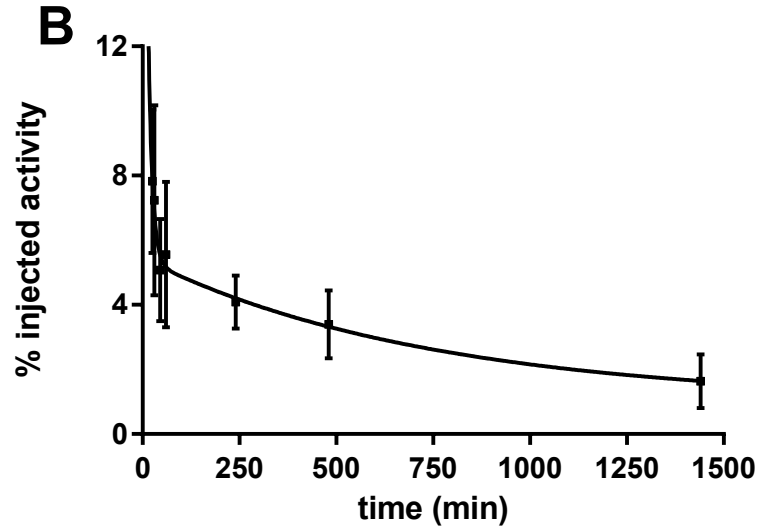
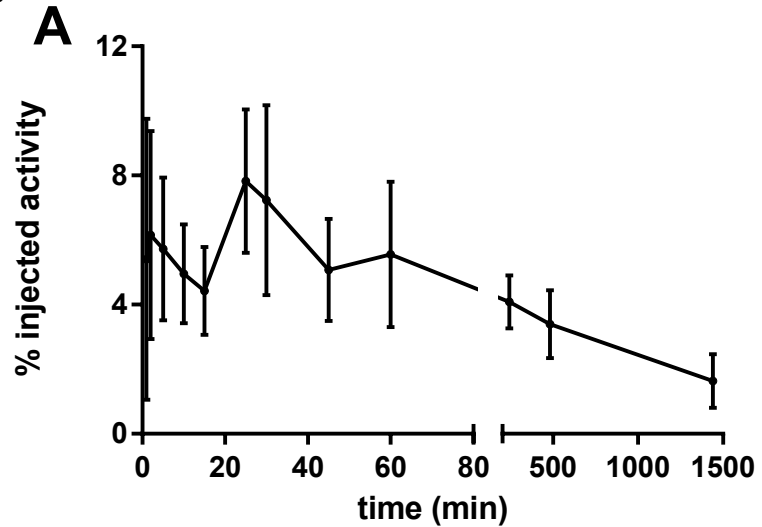


Figure 3

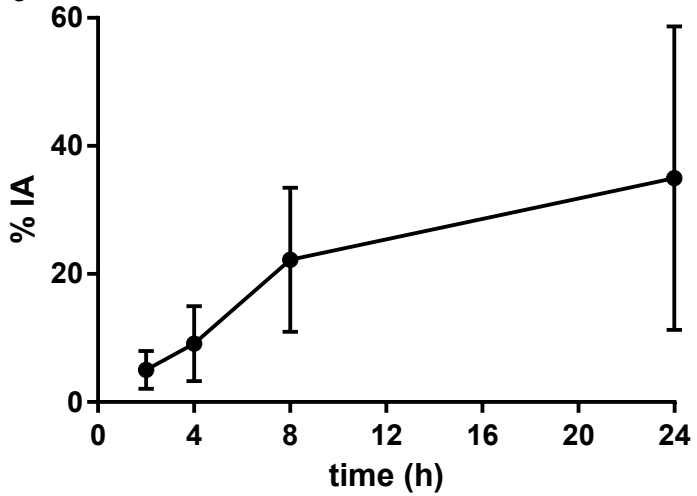
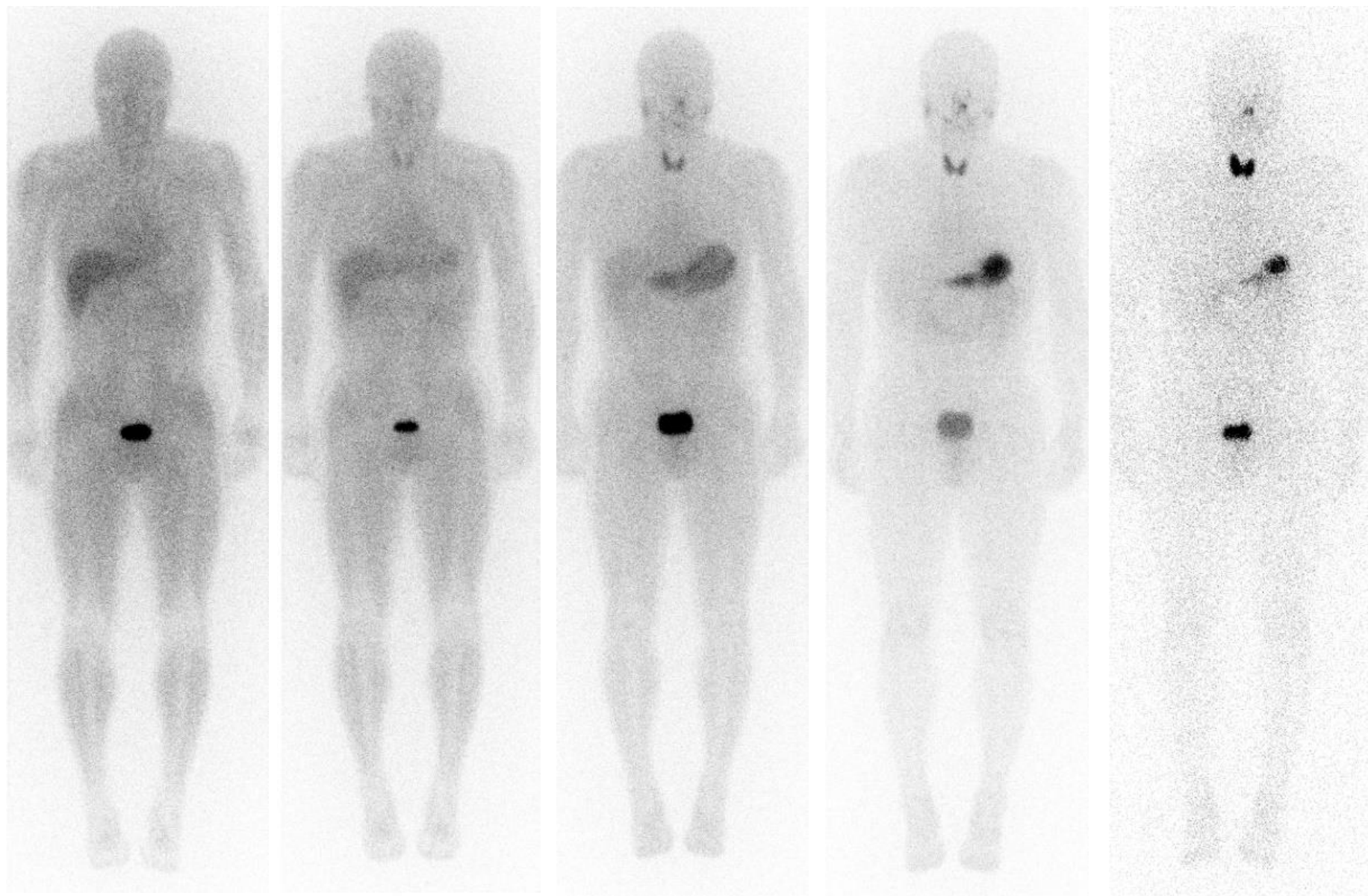


Figure 4



1H

2H

4H

8H

24H

Figure 5

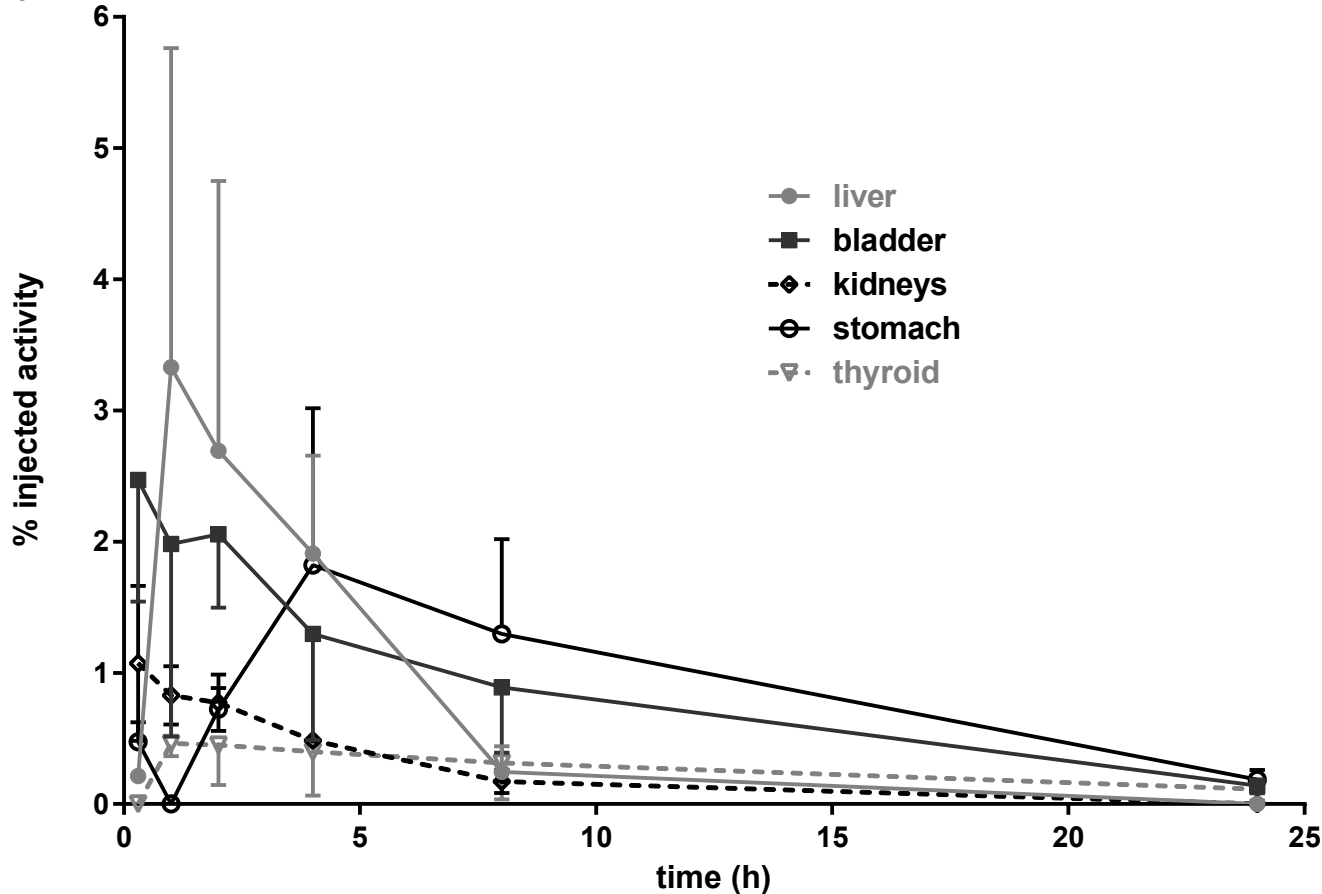


**TABLE 1.** Major characteristics of the volunteers at the time of inclusion (t1) and of 6DIG study (t2).

	<b>Glucose</b> <b>(mmol/L)</b>	<b>HbA1c</b> <b>(%)</b>	<b>Insulin</b> <b>(<math>\mu</math>IU/mL)</b>	<b>HOMA</b> <b>I*G/22.5</b>	<b>QUICKI</b> <b>1/(logI+logG)</b>
<b>Healthy t1</b>	4.6 $\pm$ 0.4 [4.1-5.3]	5.38 $\pm$ 0.22 [5.1-5.6]	2.7 $\pm$ 1.3 [0.8-4.5]	0.57 $\pm$ 0.29 [0.36-1.01]	1.03 $\pm$ 0.36 [0.74-1.73]
<b>Diabetic t1</b>	6.6 $\pm$ 0.9** [5.1-7.5]	6.7 $\pm$ 0.5** [6.2-7.6]	15.9 $\pm$ 7.7** [7.6-23.0]	4.47 $\pm$ 1.95** [2.38-7.05]	0.51 $\pm$ 0.05* [0.45-0.58]
<b>Healthy t2</b>	4.6 $\pm$ 0.3 [4.3-5.0]	nd	2.2 $\pm$ 1.0 [1.0-3.5]	0.46 $\pm$ 0.23 [0.19-0.76]	1.08 $\pm$ 0.29 [0.81-1.56]
<b>Diabetic t2</b>	6.7 $\pm$ 1.1** [5.2-8.4]	nd	24.1 $\pm$ 10.5** [8.4-37.6]	7.28 $\pm$ 3.81** [2.76-12.58]	0.47 $\pm$ 0.06** [0.41-0.56]

Data represent mean $\pm$ SD [min-max]. Comparison between healthy (n=5) and diabetic (n=6) volunteers: \* $P$ <0.05, \*\* $P$ <0.01. Comparison between t1 and t2: NS for both groups. nd: not determined.

**TABLE 2.** Frequency of adverse events (AE) reported by each volunteer during the study.

<b>System-Organ Classification MedDRA</b>	<b>AE</b>	<b>Number of subjects</b>	<b>Frequency of AE, n (%)</b>
Blood and lymphatic system disorders	Normochromic normocytic	1	1 (5.3)
Gastrointestinal disorders	Nausea	2	2 (10.5)
	Nausea		
	Vessel puncture site		
General disorders and administration site conditions	Injection site hematoma		
	Injection site hemorrhage	4	5 (26.3)
	Fatigue		
	Asthenia		
Hepatobiliary disorders	Hepatocellular injury	1	1 (5.3)
Infections and infestations	Urinary tract infection	1	1 (5.3)
Metabolism and nutrition disorders	Hyperglycemia	1	1 (5.3)
	Headache		
	Headache		
	Headache		
Nervous system disorders	Somnolence	5	7 (36.8)
	Headache		
	Headache		
	Headache		
Renal and urinary disorders	Stress urinary incontinence	1	1 (5.3)

**TABLE 3.**  $^{123}\text{I}$ -6DIG residence times in major organs of volunteers

<b>Organs</b>	<b>Residence time (h)</b>	
	Healthy (n=7)**	Diabetic (n=6)
<b>Thyroid</b>	0.11±0.02	0.10±0.04
<b>Liver</b>	0.21±0.06	0.14±0.07
<b>Bladder</b>	0.27±0.10	0.23±0.06
<b>Kidneys</b>	0.04±0.03	0.04±0.04
<b>Stomach</b>	0.29±0.11	0.27±0.13
<b>Other ROIs*</b>	0.05±0.03	0.08±0.08
<b>Remainder</b>	8.67±1.37	7.61±1.00

Data are mean ± SD.

\*Salivary glands, gonads, spleen, lungs, muscle, heart, brain, intestine.

\*\*N=7 since 2 of the 5 healthy volunteers came twice.

**TABLE 4.** Mean absorbed dose (mGy/MBq) for  $^{123}\text{I}$ -6DIG in men and women volunteers.

<b>Organs</b>	<b>Total Men (n=7)</b>	<b>Total Women (n=6)</b>
<b>Adrenals</b>	$7.49 \cdot 10^{-3} \pm 1.03 \cdot 10^{-3}$	$1.09 \cdot 10^{-2} \pm 1.67 \cdot 10^{-3}$
<b>Brain</b>	$5.80 \cdot 10^{-3} \pm 7.07 \cdot 10^{-4}$	$8.29 \cdot 10^{-3} \pm 1.41 \cdot 10^{-3}$
<b>Breast</b>	$4.77 \cdot 10^{-3} \pm 5.94 \cdot 10^{-4}$	$6.98 \cdot 10^{-3} \pm 1.15 \cdot 10^{-3}$
<b>Gallbladder Wall</b>	$7.65 \cdot 10^{-3} \pm 9.82 \cdot 10^{-4}$	$1.13 \cdot 10^{-2} \pm 1.50 \cdot 10^{-3}$
<b>Lower Large Intestine Wall</b>	$8.15 \cdot 10^{-3} \pm 9.43 \cdot 10^{-4}$	$1.29 \cdot 10^{-2} \pm 2.73 \cdot 10^{-3}$
<b>Small Intestine</b>	$8.02 \cdot 10^{-3} \pm 9.99 \cdot 10^{-4}$	$1.07 \cdot 10^{-2} \pm 1.68 \cdot 10^{-3}$
<b>Stomach Wall</b>	$1.92 \cdot 10^{-2} \pm 6.70 \cdot 10^{-3}$	$3.06 \cdot 10^{-2} \pm 6.32 \cdot 10^{-3}$
<b>Upper Large Intestine Wall</b>	$7.77 \cdot 10^{-3} \pm 9.97 \cdot 10^{-4}$	$1.14 \cdot 10^{-2} \pm 1.76 \cdot 10^{-3}$
<b>Heart Wall</b>	$7.42 \cdot 10^{-3} \pm 1.19 \cdot 10^{-3}$	$1.07 \cdot 10^{-2} \pm 1.59 \cdot 10^{-3}$
<b>Kidneys</b>	$8.71 \cdot 10^{-3} \pm 2.82 \cdot 10^{-3}$	$9.81 \cdot 10^{-3} \pm 3.51 \cdot 10^{-3}$
<b>Liver</b>	$5.55 \cdot 10^{-3} \pm 1.15 \cdot 10^{-3}$	$1.05 \cdot 10^{-2} \pm 1.10 \cdot 10^{-3}$
<b>Lungs</b>	$6.55 \cdot 10^{-3} \pm 8.24 \cdot 10^{-4}$	$9.89 \cdot 10^{-3} \pm 1.57 \cdot 10^{-3}$
<b>Muscle</b>	$6.21 \cdot 10^{-3} \pm 7.61 \cdot 10^{-4}$	$8.82 \cdot 10^{-3} \pm 1.44 \cdot 10^{-3}$
<b>Ovaries</b>	-	$1.19 \cdot 10^{-2} \pm 1.95 \cdot 10^{-3}$
<b>Pancreas</b>	$8.99 \cdot 10^{-3} \pm 1.53 \cdot 10^{-3}$	$1.33 \cdot 10^{-2} \pm 1.68 \cdot 10^{-3}$
<b>Red Marrow</b>	$5.72 \cdot 10^{-3} \pm 6.99 \cdot 10^{-4}$	$7.98 \cdot 10^{-3} \pm 1.30 \cdot 10^{-3}$
<b>Osteogenic Cells</b>	$2.05 \cdot 10^{-2} \pm 2.49 \cdot 10^{-3}$	$2.99 \cdot 10^{-2} \pm 5.03 \cdot 10^{-3}$
<b>Skin</b>	$4.32 \cdot 10^{-3} \pm 5.24 \cdot 10^{-4}$	$6.05 \cdot 10^{-3} \pm 1.00 \cdot 10^{-3}$
<b>Spleen</b>	$7.40 \cdot 10^{-3} \pm 1.28 \cdot 10^{-3}$	$1.07 \cdot 10^{-2} \pm 2.62 \cdot 10^{-3}$
<b>Testes</b>	$1.47 \cdot 10^{-2} \pm 1.46 \cdot 10^{-2}$	-
<b>Thymus</b>	$6.51 \cdot 10^{-3} \pm 8.07 \cdot 10^{-4}$	$9.48 \cdot 10^{-3} \pm 1.60 \cdot 10^{-3}$
<b>Thyroid</b>	$1.16 \cdot 10^{-1} \pm 2.87 \cdot 10^{-2}$	$1.31 \cdot 10^{-1} \pm 3.44 \cdot 10^{-2}$
<b>Urinary Bladder Wall</b>	$2.16 \cdot 10^{-2} \pm 3.91 \cdot 10^{-3}$	$4.07 \cdot 10^{-2} \pm 1.13 \cdot 10^{-2}$
<b>Uterus</b>	-	$1.29 \cdot 10^{-2} \pm 2.32 \cdot 10^{-3}$
<b>Remainder</b>	$6.64 \cdot 10^{-3} \pm 8.11 \cdot 10^{-4}$	$9.48 \cdot 10^{-3} \pm 1.49 \cdot 10^{-3}$
<b>Effective dose (mSv/MBq)</b>		
<b>CIPR60</b>	$1.65 \cdot 10^{-2} \pm 2.63 \cdot 10^{-3}$	$2.01 \cdot 10^{-2} \pm 2.41 \cdot 10^{-3} *$

Data are mean  $\pm$  SD. \* $P < 0.05$ : men *versus* women.

**TABLE 5.** Mean organ absorbed doses estimated for  $^{123}\text{I}$ -6DIG (all volunteers).

<b>Organs</b>	<b>mGy/MBq</b>	<b>For IA=185 MBq (mGy)</b>
<b>Adrenals</b>	$9.20 \cdot 10^{-3} \pm 2.22 \cdot 10^{-3}$	$1.70 \pm 0.41$
<b>Brain</b>	$6.95 \cdot 10^{-3} \pm 1.66 \cdot 10^{-3}$	$1.29 \pm 0.31$
<b>Breast</b>	$5.79 \cdot 10^{-3} \pm 1.43 \cdot 10^{-3}$	$1.07 \pm 0.26$
<b>Gallbladder Wall</b>	$9.32 \cdot 10^{-3} \pm 2.2 \cdot 10^{-3}$	$1.72 \pm 0.41$
<b>Lower Large Intestine Wall</b>	$1.04 \cdot 10^{-2} \pm 0.31 \cdot 10^{-2}$	$1.92 \pm 0.58$
<b>Small Intestine</b>	$9.25 \cdot 10^{-3} \pm 1.89 \cdot 10^{-3}$	$1.71 \pm 0.35$
<b>Stomach Wall</b>	$2.44 \cdot 10^{-2} \pm 0.86 \cdot 10^{-2}$	$4.51 \pm 1.59$
<b>Upper Large Intestine Wall</b>	$9.46 \cdot 10^{-3} \pm 2.33 \cdot 10^{-3}$	$1.75 \pm 0.43$
<b>Heart Wall</b>	$8.95 \cdot 10^{-3} \pm 2.17 \cdot 10^{-3}$	$1.66 \pm 0.40$
<b>Kidneys</b>	$9.22 \cdot 10^{-3} \pm 3.07 \cdot 10^{-3}$	$1.71 \pm 0.57$
<b>Liver</b>	$7.85 \cdot 10^{-3} \pm 2.80 \cdot 10^{-3}$	$1.45 \pm 0.52$
<b>Lungs</b>	$8.09 \cdot 10^{-3} \pm 2.09 \cdot 10^{-3}$	$1.50 \pm 0.39$
<b>Muscle</b>	$7.42 \cdot 10^{-3} \pm 1.73 \cdot 10^{-3}$	$1.37 \pm 0.32$
<b>Ovaries</b>	$1.03 \cdot 10^{-2} \pm 0.23 \cdot 10^{-2}$	$1.91 \pm 0.43$
<b>Pancreas</b>	$1.10 \cdot 10^{-2} \pm 0.27 \cdot 10^{-2}$	$2.03 \pm 0.50$
<b>Red Marrow</b>	$6.76 \cdot 10^{-3} \pm 1.52 \cdot 10^{-3}$	$1.25 \pm 0.28$
<b>Osteogenic Cells</b>	$2.48 \cdot 10^{-2} \pm 0.61 \cdot 10^{-2}$	$4.59 \pm 1.13$
<b>Skin</b>	$5.12 \cdot 10^{-3} \pm 1.17 \cdot 10^{-3}$	$0.95 \pm 0.22$
<b>Spleen</b>	$8.92 \cdot 10^{-3} \pm 2.56 \cdot 10^{-3}$	$1.65 \pm 0.47$
<b>Testes</b>	$1.47 \cdot 10^{-2} \pm 1.46 \cdot 10^{-2}$	$2.72 \pm 2.70$
<b>Thymus</b>	$7.88 \cdot 10^{-3} \pm 1.94 \cdot 10^{-3}$	$1.46 \pm 0.36$
<b>Thyroid</b>	$1.23 \cdot 10^{-1} \pm 0.31 \cdot 10^{-1}$	$22.76 \pm 5.74$
<b>Urinary Bladder Wall</b>	$3.04 \cdot 10^{-2} \pm 1.26 \cdot 10^{-2}$	$5.62 \pm 2.33$
<b>Uterus</b>	$1.09 \cdot 10^{-2} \pm 0.26 \cdot 10^{-2}$	$2.02 \pm 0.48$
<b>Remainder</b>	$7.95 \cdot 10^{-3} \pm 1.85 \cdot 10^{-3}$	$1.47 \pm 0.34$
<b>Effective dose (mSv/MBq or mSv) CIPR60</b>	$1.81 \cdot 10^{-2} \pm 0.31 \cdot 10^{-2}$	$3.35 \pm 0.57$

Data are mean  $\pm$  SD. n=13: 7 males, 6 females.